

**AN EMPIRICAL METHOD FOR DETERMINING
AVERAGE SOIL INFILTRATION RATES AND RUNOFF,
POWDER RIVER STRUCTURAL BASIN, WYOMING**

U.S. GEOLOGICAL SURVEY

Water-Resources Investigations 81-76



REPORT DOCUMENTATION PAGE	1. REPORT NO.	2.	3. Recipient's Accession No.
4. Title and Subtitle AN EMPIRICAL METHOD FOR DETERMINING AVERAGE SOIL INFILTRATION RATES AND RUNOFF, POWDER RIVER STRUCTURAL BASIN, WYOMING		5. Report Date April 1982	
7. Author(s) J. G. Rankl		6.	
9. Performing Organization Name and Address U.S. Geological Survey, Water Resources Division 2120 Capitol Avenue Cheyenne, Wyoming 82001		8. Performing Organization Rept. No. USGS/WRI 81-76	
12. Sponsoring Organization Name and Address U.S. Geological Survey, Water Resources Division 2120 Capitol Avenue Cheyenne, Wyoming 82001		10. Project/Task/Work Unit No.	
		11. Contract(C) or Grant(G) No. (C) (G)	
		13. Type of Report & Period Covered Final	
15. Supplementary Notes		14.	
16. Abstract (Limit: 200 words) This report describes a method to estimate infiltration rates of soils for use in estimating runoff from small basins. Average rainfall intensity is plotted against storm duration on log-log paper. All rainfall events are designated as having either runoff or nonrunoff. A power-decay-type curve is visually fitted to separate the two types of rainfall events. This separation curve is an incipient-ponding curve and its equation describes infiltration parameters for a soil. For basins with more than one soil complex, only the incipient-ponding curve for the soil complex with the lowest infiltration rate can be defined using the separation technique. Incipient-ponding curves for soils with infiltration rates greater than the lowest curve are defined by ranking the soils according to their relative permeabilities and optimizing the curve position. A comparison of results for six basins produced computed total runoff for all events used ranging from 16.6 percent less to 2.3 percent more than measured total runoff.			
17. Document Analysis a. Descriptors *Antecedent moisture, *Infiltration, *Rainfall intensity, Soil groups, Surface runoff, Wyoming. b. Identifiers/Open-Ended Terms Channel storage, Incipient ponding, Separation curve, Water uptake, Powder River basin. c. COSATI Field/Group			
18. Availability Statement: No restriction on distribution		19. Security Class (This Report)	21. No. of Pages 43
		20. Security Class (This Page)	22. Price

AN EMPIRICAL METHOD FOR DETERMINING AVERAGE SOIL INFILTRATION
RATES AND RUNOFF, POWDER RIVER STRUCTURAL BASIN, WYOMING

By J. G. Rankl

U.S. GEOLOGICAL SURVEY

Water-Resources Investigations 81-76



April 1982

UNITED STATES DEPARTMENT OF THE INTERIOR

JAMES G. WATT, Secretary

GEOLOGICAL SURVEY

Dallas L. Peck, Director

For additional information write to:

District Chief
U.S. Geological Survey
2120 Capitol Avenue
P.O. Box 1125
Cheyenne, Wyoming 82001

CONTENTS

	Page
Abstract-----	1
Introduction-----	2
Objective and approach-----	2
Basin descriptions-----	2
Data requirements-----	4
Development of theory-----	4
Incipient ponding-----	4
Infiltration curves-----	6
Comparison to Horton's equation-----	7
Computation of runoff-----	10
Analysis of data for a single-soil complex-----	10
Sensitivity of parameters-----	18
Test of constant rainfall rate-----	18
Basins with multiple-soil complexes-----	20
Soil-complex ranking-----	22
Analysis of data for multiple-soil complexes-----	26
Long-term comparison-----	32
Summary-----	37
References cited-----	38

ILLUSTRATIONS

Figure 1. Map showing location of partial-record stations used in this report-----	3
2. Incipient-ponding curve from rainfall and runoff data-----	5
3. Graph showing comparison of equation 3 with Horton's infiltration equation (eq 5)-----	9
4. Infiltration curves derived from the incipient- ponding curve-----	11
5-7. Incipient-ponding curve and equation	
5. Dugout Creek tributary near Midwest, Wyo. (06313180)-----	17
6. Dead Horse Creek tributary near Midwest, Wyo. (06312910)-----	17
7. Dead Horse Creek tributary No. 2 near Midwest, Wyo. (06312920)-----	17
8. Graphs showing incipient-ponding curves for changes in indicated parameters, Dugout Creek tributary near Midwest, Wyo. (06313180)-----	19
9. Schematic model of subbasin infiltration rates-----	21
10. Soil maps of basins used in this study-----	25
11-13. Lowest incipient-ponding curve and equation	
11. Frank Draw tributary near Orpha, Wyo. (06648720)-----	27
12. Sage Creek tributary near Orpha, Wyo. (06648780)-----	27
13. Headgate Draw at upper station near Buffalo, Wyo. (06316480)-----	27

ILLUSTRATIONS--Continued

	Page
Figure 14. Incipient-ponding curves for Frank Draw tributary near Orpha, Wyo. (06648720)-----	28
15. Incipient-ponding curves for Sage Creek tributary near Orpha, Wyo. (06648780)-----	29
16. Comparison of optimized incipient-ponding curves for soils common to both Frank Draw tributary near Orpha, Wyo. (06648720) and Sage Creek tributary near Orpha, Wyo. (06648780)-----	30
17. Incipient-ponding curves for Headgate Draw at upper station, near Buffalo, Wyo. (06316480)-----	31
18. Graphs showing comparison of results of long-term simulated runoff data using two simulation methods for Dugout Creek tributary near Midwest, Wyo. (06313180), Dead Horse Creek tributary near Midwest, Wyo. (06312910), Dead Horse Creek tributary No. 2 near Midwest, Wyo. (06312920), Frank Draw tributary near Orpha, Wyo. (06648720), Sage Creek tributary near Orpha, Wyo. (06648780), and Headgate Draw at upper station near Buffalo, Wyo. (06316480)-----	36

TABLES

Table 1. Precipitation and runoff data for Dugout Creek tributary near Midwest, Wyo. (06313180)-----	13
2. Precipitation and runoff data for Dead Horse Creek tributary near Midwest, Wyo. (06312910)-----	14
3. Precipitation and runoff data for Dead Horse Creek tributary no. 2 near Midwest, Wyo. (06312920)-----	15
4. Comparison of computed runoff to measured runoff for small basins with homogeneous soils-----	16
5. Relative class values of soil permeability-----	23
6. Sample computation to determine composite relative permeability index for the Terry-Tulloch-Valent soil complex-----	23
7. Mapping units for soil maps and associated permeabilities-----	24
8. Soil parameters for incipient-ponding curves in the Powder River Basin-----	33
9. Precipitation and runoff data for Sage Creek tributary near Orpha, Wyo. (06648780)-----	34
10. Precipitation and runoff data for Frank Draw tributary near Orpha Wyo. (06648720)-----	34
11. Precipitation and runoff data for Headgate Draw at upper station near Buffalo, Wyo. (0631480)-----	35
12. Comparison of computed runoff to measured runoff for small basins with multiple soils-----	35

SYMBOLS

a	Constant for a soil type, in millimeters.
f_c	Saturated hydraulic conductivity, in millimeters per hour.
f_o	Horton's maximum infiltration rate.
I	Infiltration rate, in millimeters per hour.
I_p	Infiltration rate at time of incipient ponding, in millimeters per hour.
I_s	Average intensity of rainfall, in millimeters per hour.
k	Empirical constant associated with a soil complex.
n	Exponent parameter.
n_1	Number of simulated events.
R_t	Total simulated runoff.
t	Time from beginning of storm, in hours.
t_h	Horton's t , time in hours.
t_p	Time to incipient ponding for a given intensity, in hours.
s^2	Variance
SSE	Sum of the squared deviations.
y_i	Simulated runoff values.
\hat{y}_i	Measured runoff values.
W_u	Total water uptake, in millimeters.

AN EMPIRICAL METHOD FOR DETERMINING AVERAGE SOIL INFILTRATION RATES
AND RUNOFF, POWDER RIVER STRUCTURAL BASIN, WYOMING

By J. G. Rankl

ABSTRACT

This report describes a method to estimate infiltration rates of soils for use in predicting runoff from small basins containing these soils. Data requirements are: (1) Rainfall frequency, (2) soils maps, and (3) rainfall-runoff data. The emphasis of this report is development of the theory and verification of the method.

Three simplifying assumptions are: (1) Initial water uptake includes interception by vegetation, surface storage, and channel storage; (2) some average antecedent moisture condition exists; and (3) rainfall for a storm event is uniform both in space and time.

Average rainfall intensity is plotted against storm duration on log-log paper. All rainfall events are designated as runoff or nonrunoff events. A power-decay-type curve is visually fitted to separate the two types of rainfall events. This separation curve is an incipient-ponding curve and its equation describes infiltration parameters for a soil. The parameters are used to define a series of infiltration-rate curves for that soil.

For basins with more than one soil complex, only the incipient-ponding curve for the soil complex with the lowest infiltration rate can be defined using the separation technique. Incipient-ponding curves for soils with infiltration rates greater than the lowest curve are defined by ranking the soils according to their relative permeabilities and optimizing curve position using measured runoff as a control for the fit.

A comparison was made between the sums of computed runoff and of measured runoff for all available runoff events in the six basins studied. Summation of the computed runoff events ranged from 16.6 percent less to 2.3 percent more than the summation of the measured runoff events.

INTRODUCTION

Knowledge of the infiltration of rainfall into soils and of the excess precipitation from a storm has taken on an additional importance with the passage of the Surface Mining Control and Reclamation Act of 1977. In addition to requiring restoration of the approximate original infiltration rate and capacity, the rules and regulations of the Act require that water-impoundment and drainage structures be designed using precipitation-frequency criteria. Past studies that provided design information for structures were based on regression analysis relating physical basin parameters to runoff frequency. The relation between storm frequency and runoff frequency has not been determined.

Most infiltration studies have used one of three approaches: (1) Physics of flow in the unsaturated zone, (2) infiltrometer samples, or (3) soil-index methods. The first approach has provided the theory and knowledge of the infiltration processes but is seldom applicable to field conditions without a detailed data-collection program to define the necessary soil parameters. The relation between infiltration rates obtained from an infiltrometer test and the infiltration rates that affect the runoff from small basins has not been fully demonstrated. Soil-index methods approach the infiltration-runoff problem from a basin aspect but fail to take rainfall intensity into account.

Objective and Approach

The objective of this study was to develop a method for determining infiltration rates and the associated runoff for selected soil groups. Three steps were taken to determine infiltration rates: (1) An incipient-ponding curve was determined from rainfall-runoff data, (2) an infiltration curve was developed from soil parameters as determined from the incipient-ponding curve, and (3) a method was developed to assign infiltration rates to soil subareas for each basin.

Basin Descriptions

Rainfall and runoff data from 22 small drainage basins were available for the study. Data from six of the small basins were analyzed in detail to verify the method. The six basin sizes ranged from 1.84 km² (square kilometers) to 8.60 km². Three of the basins have a uniform soil type underlain by the Cody Shale of Cretaceous age, and three of the basins are multisoiled, underlain by the Wasatch Formation of Eocene age.

Locations of stations and their station numbers are shown in figure 1. Partial-record stations that appear in this report have been assigned an 8-digit number. The 8-digit number consists of two parts: The first two digits are the drainage-basin numbers and the remaining six digits are the station number. The station numbers increase in a downstream direction.

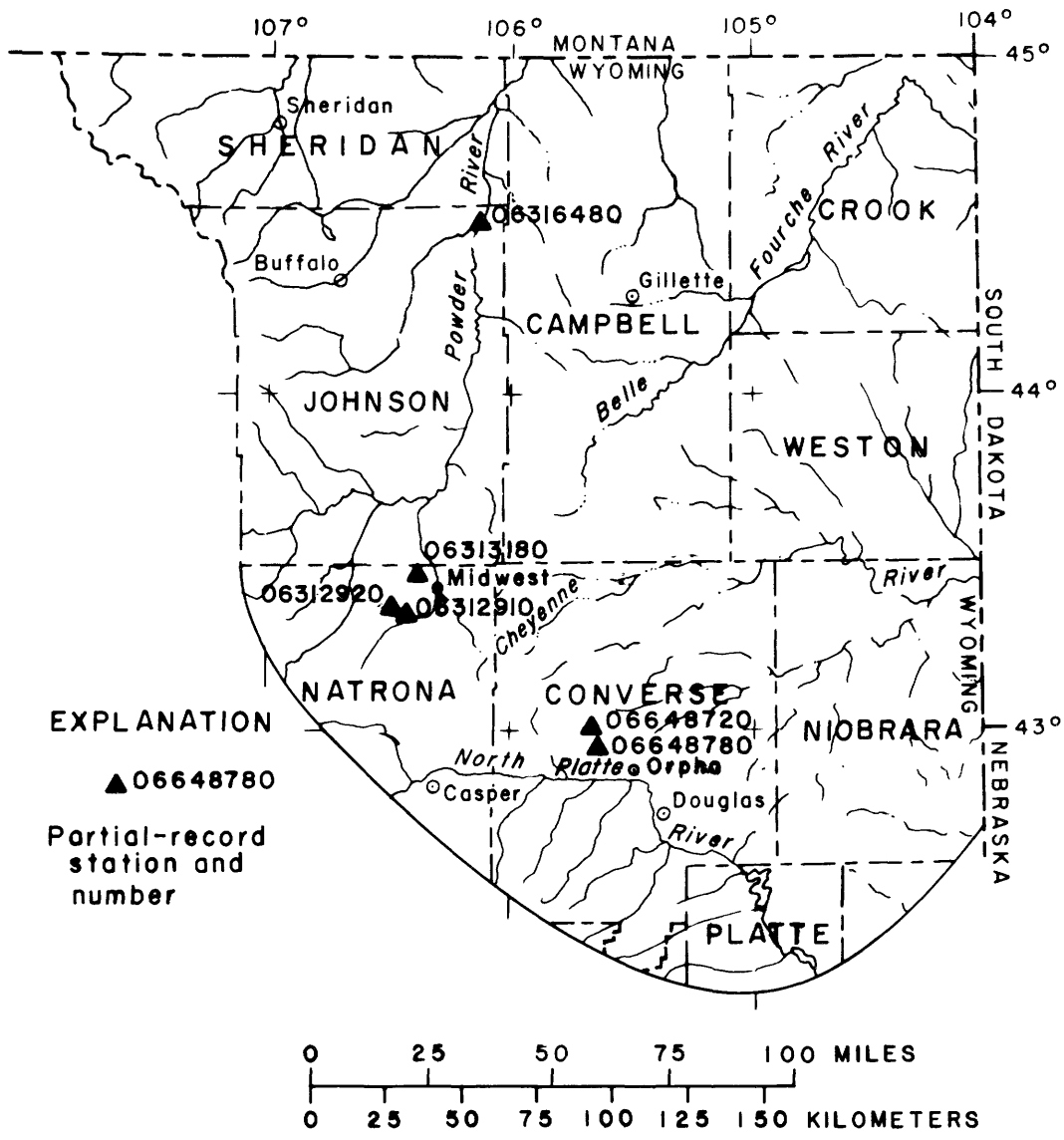


Figure 1.--Location of partial-record stations used in this report.

DATA REQUIREMENTS

Recorded rainfall and runoff data are required for the analysis. Average storm intensity and storm length must be computed for each event used, and the storm event must be designated as a runoff or nonrunoff event. The total volume for each runoff event is used to check the method and is needed to determine infiltration in basins with multiple soils. Rainfall-runoff data analyzed in this report were collected by the U.S. Geological Survey from 1965 to 1973 at streamflow stations on small, ephemeral streams having drainage areas of less than 28.5 km² (Craig and Rankl, 1978).

Soil maps are needed for each basin with more than one soil type to determine the area of each soil. In addition, a description of the soils is needed to determine the potential infiltration rate of each soil complex or association. The potential infiltration rates are used to rank the soils relative to each other. It is important that the mapping units be consistent; therefore, soil maps and descriptions for the study were obtained from the U.S. Department of Agriculture, Soil Conservation Service.

DEVELOPMENT OF THEORY

Incipient Ponding

Given a constant rainfall flux, incipient ponding can be defined as the state in which the rainfall rate is equal to the infiltration rate and free water begins to form at the soil surface. Theory and definitions of incipient ponding were given by Rubin (1966), and Smith (1972), and Swartzendruber and Hillel (1975).

In this report, the definition of incipient ponding is expanded to include the beginning of runoff. The term "incipient ponding" is retained in order to relate infiltration after ponding to the incipient-ponding curve. Several assumptions are needed for the expanded definition. First: Interception, surface storage, and channel storage are included in the water uptake from the time (t_0) at the beginning of the storm to the time of ponding (t_p). Second: The soil-moisture condition at the time of the storm is some long-term average value. Third: The rainfall for a given storm is uniform in both space and time.

Given these assumptions an incipient-ponding curve for a small basin with a single soil type can be defined by plotting rainfall intensities, in millimeters per hour (mm/h), on the y-axis and the length of the storm, in hours, on the x-axis (M. E. Lowry, U.S. Geological Survey, written commun., 1973). Each storm is designated as a runoff or nonrunoff event (fig. 2). The best-fit line that separates the runoff and nonrunoff events based on the data points is the incipient-ponding curve for the soil.

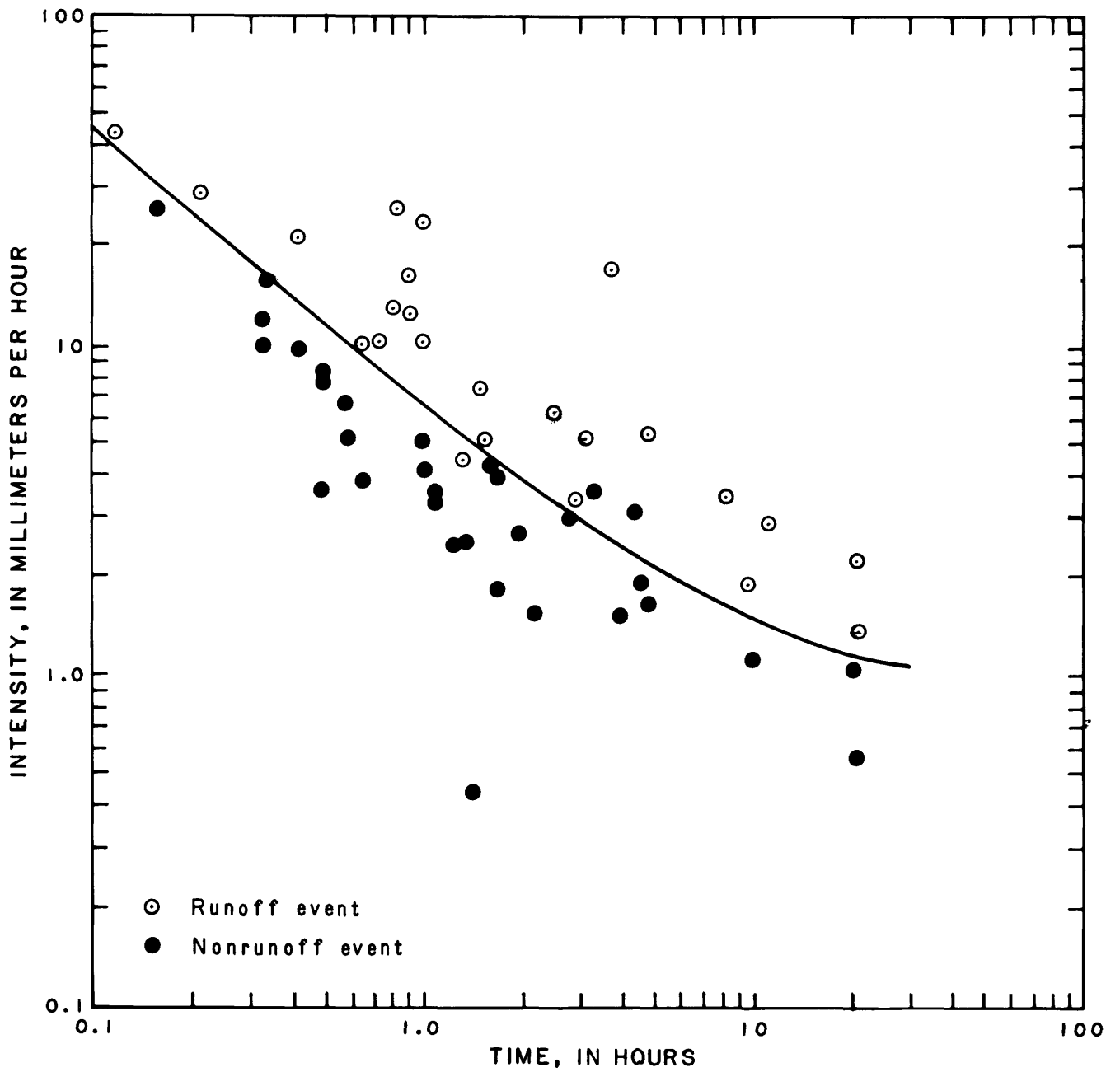


Figure 2.--Incipient-ponding curve from rainfall-runoff data.

Data from the 22 small basins were used to determine a type equation that would best fit the data for all the basins. Rubin (1966, fig. 7) and Smith (1972, fig. 5) described ponding time-intensity relations with power-decay-type curves. These curves worked well with high-intensity, short-duration storms but failed to define the separation between runoff and nonrunoff events of low intensity and long duration. That is, when the rainfall intensity of the events approached the saturated hydraulic conductivity value, the separation curve was too low. An infiltration equation described by Swartzendruber and Hillel (1975), which is a power-decay-type equation with a constant added for saturated hydraulic conductivity, defined the separation curve between runoff and nonrunoff events. The following equation best describes the incipient-ponding curve:

$$I_p = a t^{-n} + f_c \quad (1)$$

where I_p is the rate of infiltration when the rainfall flux equals infiltration rate, in millimeters per hour;
 a is a constant for a soil type, in millimeters;
 t is time, in hours;
 n is an exponent parameter; and
 f_c is the saturated hydraulic conductivity, in millimeters per hour.

Equation 1 was fitted mathematically by trial and error using different combinations of values for a , n , and f_c . The best fit was determined visually. For the 22 basins studied, preliminary values for a ranged from 2.41 mm to 7.12 mm, values for f_c ranged from 0.25 mm/h to 1.25 mm/h, and values for n ranged from 0.72 to 0.98. The mean of the values for n was 0.87.

Infiltration Curves

Previous works on infiltration have defined the incipient-ponding curve from a series of infiltration curves for a constant initial soil-moisture content. In this investigation, the soil parameters as determined by the incipient-ponding curve were used to develop an infiltration curve after ponding. Rainfall and runoff data were used to test the validity of the equations.

Time of incipient ponding can be computed from equation 1. Assuming that the rainfall flux (I_s) is equal to the infiltration rate (I_p) at time t_p , equation 1 can be rearranged to become

$$t_p = \left[\frac{I_s - f_c}{a} \right]^{-1/n} \quad (2)$$

where t_p is time to ponding, in hours, and
 I_s is rainfall flux, in millimeters per hour.

This equation is similar to equation 8 of Smith and Chery (1973, p.1342) which describes the infiltrated volume at the time of ponding.

Variable a is assumed to be a function of the maximum volume of moisture that a unit area of soil can hold with an average antecedent moisture state. At time t , the surface layer of the soil becomes saturated, and then the rate of infiltration is controlled by the remaining unfilled volume of the soil column. As rainfall continues, the ability of the soil to store additional infiltrated moisture approaches zero and the rate of infiltration approaches the saturated hydraulic conductivity (f_c). A change in the soil-moisture relationship as time increases is described by a ratio of the infiltrated moisture in the soil column to the maximum volume of moisture the soil can hold. If the computed change in the infiltration rate is based on the change in the accumulated moisture, an iteration technique is required. The solution for the decrease in infiltration rate can be evaluated directly if the decrease is a function of time. A time function can be used if the rainfall flux is uniform in space and time. The infiltration equation must evaluate the rate of precipitation uptake from time t_p to the end of the storm; therefore, the infiltration equation and the incipient-ponding equation must be equal at time t_p . With the above assumptions and considerations, an infiltration equation based on the incipient-ponding equation can be written as

$$I = a \left[\frac{t - t_p}{t} \right] t^{-n} + f_c \quad (3)$$

where $t \geq t_p$.

Equation 3 can then be expressed as

$$I = a t_p t^{-(n+1)} + f_c \quad (4)$$

Comparison to Horton's Equation

A comparison of the results using equation 3 was made with the results obtained using Horton's infiltration equation as given by Linsley and others (1958, p. 166), which is

$$f = f_c + (f_o - f_c) e^{-kt_h} \quad (5)$$

where f is rate curve for infiltration capacity;

f_c is a low constant rate when the soil profile is saturated;

f_o is the maximum infiltration rate at t equals 0;

t_h is time from the beginning of the event; and

k is an empirical constant associated with a soil complex.

Horton's equation is based on the assumption that $I_s \geq f_c$; therefore, the equation is applicable only at or after t_p , the time of incipient ponding (Linsley and others, 1958, p. 166). A comparison of parameters can be made between equations 3 and 5. The values for f_c should be equal. The beginning infiltration rate of Horton's f_c can be equated to the rate at incipient ponding (I_p) at time t_p . Time $t_h = 0$ in Horton's equation can be equated to time t_p in equation 2. A comparison of the two equations is made using parameters from the incipient-ponding curve with $a = 3.81$, $f_c = 0.508$, $n = 0.80$, $k = 2.20$ (assumed) and Horton's $t_h = t - t_p$. The incipient-ponding curve, the infiltration curve from equation 3, and Horton's equation (eq 5) based on parameters values from the incipient-ponding curve are shown in figure 3.

Horton's soil-complex number (k) controls the slope of the decay curve as does n in equation 3. The soil complex number (k) can be expressed in terms of n and time if equations 4 and 5 are assumed to be approximately equal. This can be done by setting the equations equal to each other and solving for k in terms of n and time t .

$$f_c + (f_o - f_c) e^{-kt_h} = a t_p t^{-(n+1)} + f_c \quad (6)$$

$$f_o = I_p = a t_p^{-n} + f_c \quad (7)$$

$$\text{Horton's } t_h = t - t_p \quad (8)$$

$$(a t_p^{-n} + f_c - f_c) e^{-k(t-t_p)} = a t_p t^{-(n+1)} \quad (9)$$

$$e^{-k(t-t_p)} = \frac{t_p t^{-(n+1)}}{t_p^{-n}} \quad (10)$$

$$-k(t-t_p) = \ln (t_p^{n+1} t^{-(n+1)}) \quad (11)$$

$$k = \frac{(n+1)(\ln t - \ln t_p)}{(t - t_p)} \quad (12)$$

Horton's k becomes a variable as a function of both time and n from equation 3. Values of k computed from equation 12 for $t_p = 0.1$, $n = 0.80$, $f_o = 24.55$, and $f_c = 0.508$ are listed below:

<u>Time,</u> <u>in hours</u>	<u>k</u>
0.2	12.48
.5	7.24
1.0	4.61
2.0	2.83
5.0	1.44

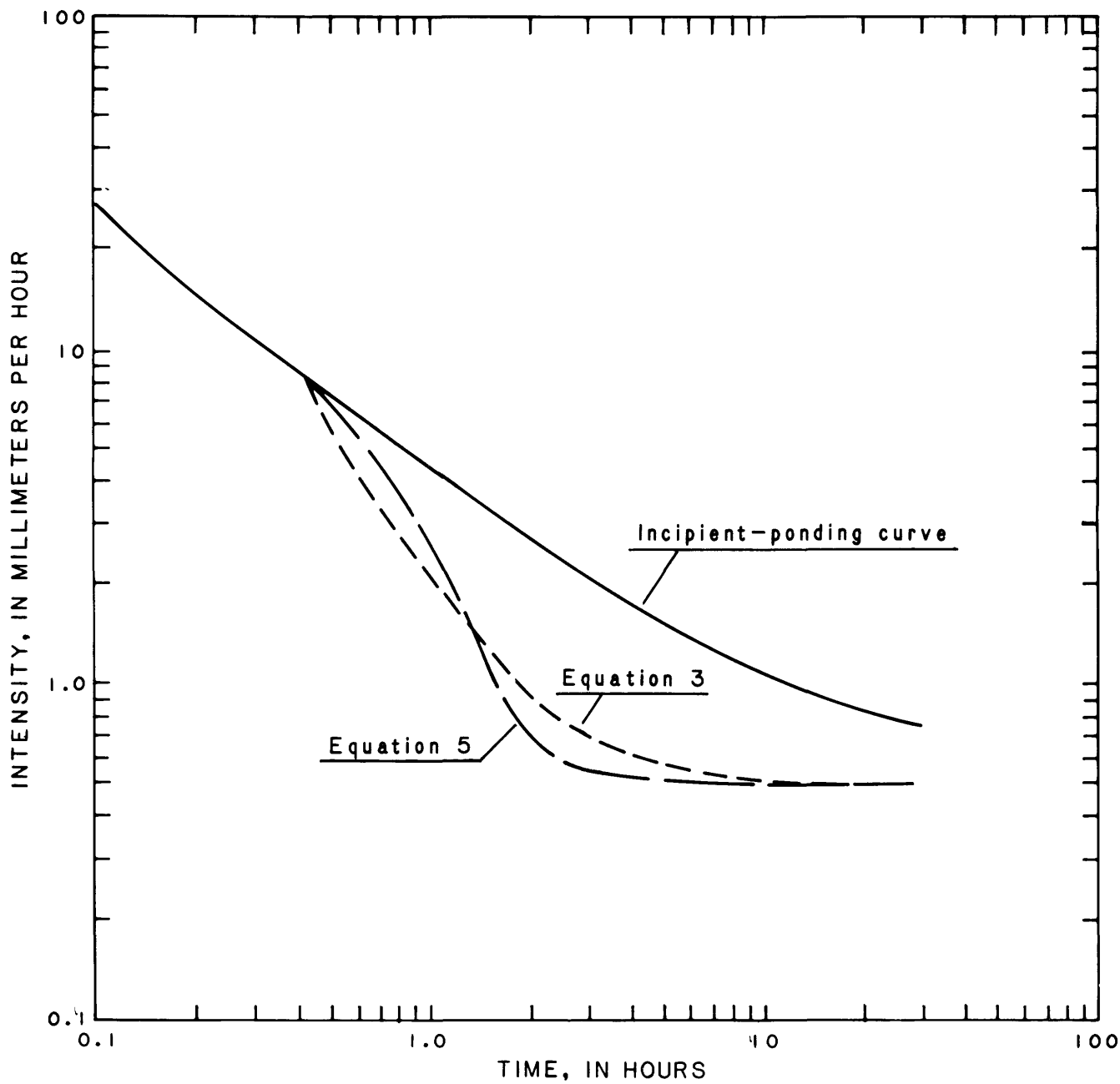


Figure 3.--Comparison of equation 3 with Horton's infiltration equation (eq 5).

These results are well within the range of Horton's value for k (Musgrave and Holtan, 1964, fig. 12-8).

Computation of runoff

Water uptake (W_u) for a rainfall with a 20-hour duration and an average intensity of 2.0 millimeters per hour is shown by the shaded area in figure 4. Total water uptake can then be computed as

$$W_u = \int_{t_p}^t (a t_p t^{-(n+1)} + f_c) dt + I_s t_p. \quad (13)$$

Integration of equation 13 yields

$$W_u = -\frac{a t_p}{n} (t^{-n} - t_p^{-n}) + f_c (t - t_p) + I_s t_p. \quad (14)$$

Total runoff (R_t) can be computed by subtracting the total water uptake from total rainfall for the storm:

$$R_t = I_s t - W_u. \quad (15)$$

ANALYSES OF DATA FOR A SINGLE-SOIL COMPLEX

Three small basins, Dugout Creek tributary near Midwest, Wyo. (06313180), Dead Horse Creek tributary near Midwest, Wyo. (06312910), and Dead Horse Creek tributary No. 2 near Midwest, Wyo. (06312920) are located in northern Natrona County, Wyo., in an area underlain by the Cody Shale. These basins have not been mapped for soil types, but a few kilometers north, in southern Johnson County, Wyo., soil maps and descriptions (Stephens, 1975) are available for soils derived from the Cody Shale.

Soils mapped in areas underlain by the Cody Shale are tight clays, clay loams, and areas mapped as badlands. In any case, the soils developed on the Cody Shale have a very low permeability and a high shrink-swell potential; they are strongly alkaline and moderately salty. The basins studied in this area may have several soil types, but they are considered to have one common, low infiltration rate.

Incipient-ponding curves for these basins were developed by plotting rainfall intensity against storm duration for runoff and nonrunoff events

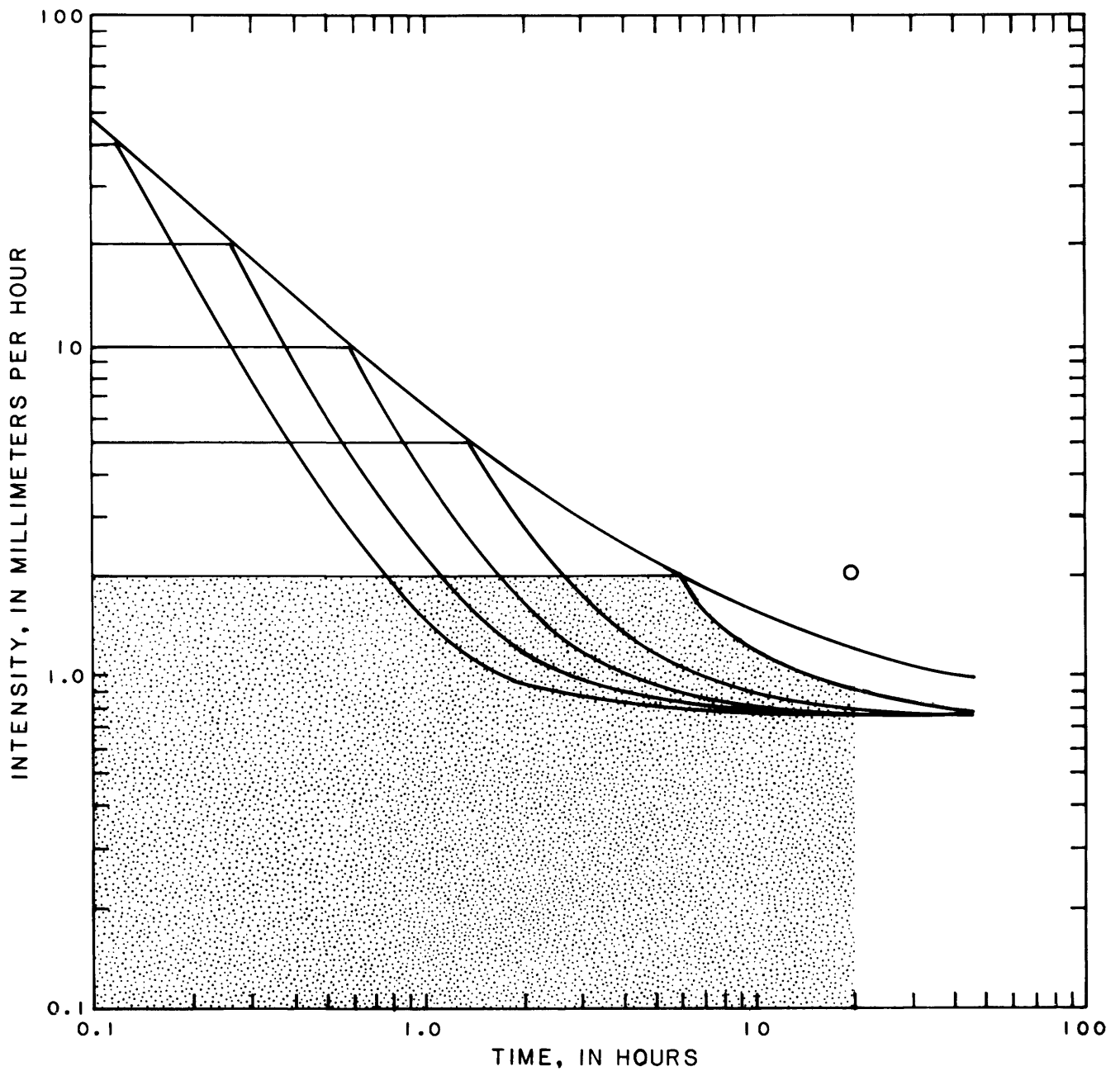


Figure 4.--Infiltration curves derived from incipient-ponding curve. Shaded area is example given in text.

and constructing the separation curves. The incipient-ponding curve and equation for Dugout Creek tributary near Midwest, Wyo. (06313180) are shown in figure 5, Dead Horse Creek tributary near Midwest, Wyo. (06312910) in figure 6, and Dead Horse Creek tributary No. 2 near Midwest, Wyo. (06312920) in figure 7. Data determined by the incipient-ponding curves were used with equations 2, 14, and 15 to simulate the runoff from rainfall events with known volumes. The date, total rainfall, storm duration, storm intensity, measured runoff, and simulated runoff of each event for the above stations are listed in tables 1, 2, and 3.

Because an objective of this study was to define an average infiltration curve for a given soil complex with an average antecedent condition, the summation of computed runoff for all the usable events for a basin was compared to the total measured runoff of all the events. Individual events were compared by computing the standard deviation of the measured events and the simulated events. These comparisons are summarized in table 4 for the three basins.

An estimate of the variance was computed by dividing the sum of the squares of the deviations by the number of events, minus 2 degrees of freedom. The standard deviation was computed by taking the square root of variance.

$$SSE = \sum_{i=1}^n (y_i - \hat{y}_i)^2 \quad (16)$$

where SSE = sum of the squared deviations,
n = number of simulated events,
 y_i = the simulated runoff value,
 \hat{y}_i = measured runoff value, and
S = standard deviation.

$$S = \sqrt{\frac{SSE}{n-2}} \quad (17)$$

The relatively large values of the standard deviations for the small basins can be partly explained by the difference in antecedent moisture conditions. Craig and Rankl (1978, p. 19) found that runoff from small basins is sensitive to antecedent conditions. In this study, an average antecedent-moisture condition is assumed so it is possible to apply a design-storm event to the infiltration equations when the antecedent conditions are not known.

Table 1.--Precipitation and runoff data for Dugout Creek tributary
near Midwest, Wyo. (06313180)

Date	Rainfall (mm)	Length of storm (h)	Intensity (mm/h)	Measured runoff (mm)	Simulated runoff (mm)
05-23-65	12.45	0.92	13.53	4.06	6.01
06-24-65	23.11	4.08	5.66	12.75	13.56
07-01-65	7.62	.17	44.82	4.06	2.75
09-01-66	12.70	2.75	4.62	4.29	4.56
06-09-67	7.62	1.33	5.73	2.54	1.35
06-13-67	6.35	2.67	2.38	2.21	.05
06-14-67	7.37	.92	8.01	3.75	1.50
06-15-67	35.54	6.75	5.27	23.62	23.99
09-18-67	11.68	2.67	4.37	5.97	3.71
09-26-67	2.29	.42	5.45	.64	1.32
06-05-68	5.59	1.08	5.18	.79	.27
06-06-68	10.41	5.58	1.87	3.07	.91
09-03-68	10.41	3.33	3.13	5.86	2.16
06-19-69	5.59	.25	22.35	1.07	.93
05-22-70	31.75	4.25	7.47	19.15	22.09
05-24-70	14.99	1.17	12.81	6.17	8.18
05-30-70	5.08	.50	10.10	1.02	.34
06-17-72	5.59	.17	32.88	.74	1.08
06-18-72	7.37	.92	8.01	2.45	1.50
09-19-72	14.48	2.75	5.27	9.65	6.33
06-30-72	4.57	.50	9.14	1.45	.13
08-02-72	8.64	1.67	5.17	3.48	1.88
08-24-72	38.86	6.08	6.39	24.00	27.80
09-11-72	3.56	.42	8.48	1.19	.01

Table 2.--Precipitation and runoff data for Dead Horse Creek tributary
near Midwest, Wyo. (06312910)

Date	Rainfall (mm)	Length of storm (h)	Intensity (mm/h)	Measured runoff (mm)	Simulated runoff (mm)
06-16-65	11.43	0.83	13.77	7.42	5.01
09-13-66	5.84	.67	8.72	1.45	.58
09-14-66	5.33	1.00	5.33	.66	.17
06-15-67	33.27	7.00	4.75	23.85	22.48
06-23-67	28.70	13.00	2.21	18.19	14.88
07-12-67	10.41	.33	31.54	.48	4.73
07-15-67	8.38	.17	49.29	.46	3.22
07-18-67	7.37	1.66	4.44	.46	.99
09-18-67	8.38	3.92	2.14	1.68	.73
05-22-68	10.41	10.00	1.04	1.19	.19
05-23-68	19.56	8.50	2.30	7.34	8.13
05-23-68	8.64	2.66	3.25	5.31	1.40
06-06-68	13.97	11.66	1.20	10.49	1.81
06-06-68	3.30	1.00	3.30	2.25	.00
06-07-68	5.59	1.50	3.73	4.55	.13
05-22-70	11.18	.50	22.30	2.31	5.18
08-09-71	5.33	.17	31.35	.15	.76
06-03-72	31.24	1.00	31.24	28.30	24.47
06-03-72	10.16	1.08	9.41	9.88	3.62
08-02-72	20.07	4.58	4.38	8.56	10.70
08-24-72	27.18	10.25	2.65	13.49	14.69

Table 3.--Precipitation and runoff data for Dead Horse Creek tributary No. 2
near Midwest, Wyo. (06312920)

Date	Rainfall (mm)	Length of storm (h)	Intensity (mm/h)	Measured runoff (mm)	Simulated runoff (mm)
05-23-65	5.59	1.58	3.54	1.09	0.01
07-05-65	8.64	2.58	3.35	2.51	1.07
07-25-65	4.83	.75	6.44	1.17	.00
06-22-66	13.21	.75	17.61	3.45	6.07
09-01-66	11.18	1.58	7.08	3.30	3.55
09-01-66	10.41	2.25	4.63	3.71	2.52
06-07-67	3.05	.08	36.75	1.50	.13
06-14-67	5.33	1.00	5.33	1.83	.03
06-14-67	33.27	11.83	2.81	12.40	20.00
06-20-67	3.05	.42	7.26	2.69	.00
06-20-67	8.89	.42	21.17	5.84	2.60
06-22-67	9.91	2.83	3.50	3.05	1.86
06-22-67	16.51	8.17	2.02	5.10	5.27
07-15-67	11.68	.58	20.14	6.65	4.85
06-07-68	6.10	.50	12.20	2.36	.51
07-20-69	2.29	.17	13.47	.38	.00
08-09-71	7.87	.17	46.29	3.02	2.23
06-19-72	11.68	3.33	3.51	2.95	3.06
08-02-72	10.92	2.50	4.37	.76	2.81
08-02-72	8.89	1.42	6.26	1.45	1.77
08-24-72	24.64	5.58	4.42	5.66	14.19

Table 4.--Comparison of computed runoff to measured runoff for small basins with

homogeneous soils

Basin name and number	Number of events	Total rainfall (mm)	Measured runoff (mm)	Computed runoff (mm)	Percent difference	Standard deviation
Dugout Creek tributary near Midwest, Wyo. (06313180)	24	293.6	144.0	132.4	- 8.1	2.00
Dead Horse Creek tributary near Midwest, Wyo. (06312910)	21	285.7	148.5	123.9	-16.6	3.50
Dead Horse Creek tributary No. 2 near Midwest, Wyo. (06312920)	21	217.9	70.9	72.5	+ 2.3	3.08

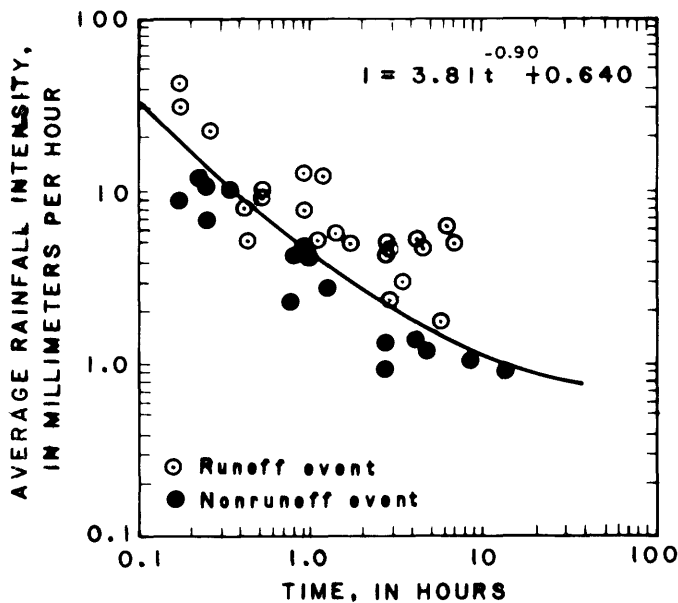


Figure 5.--Incipient-ponding curve and equation, Dugout Creek tributary near Midwest, Wyoming (06313180).

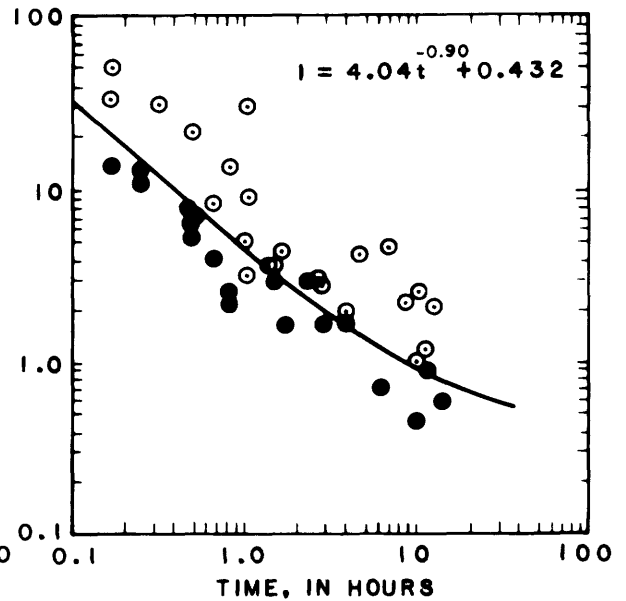


Figure 6.--Incipient-ponding curve and equation, Dead Horse Creek tributary near Midwest, Wyoming (06312910).

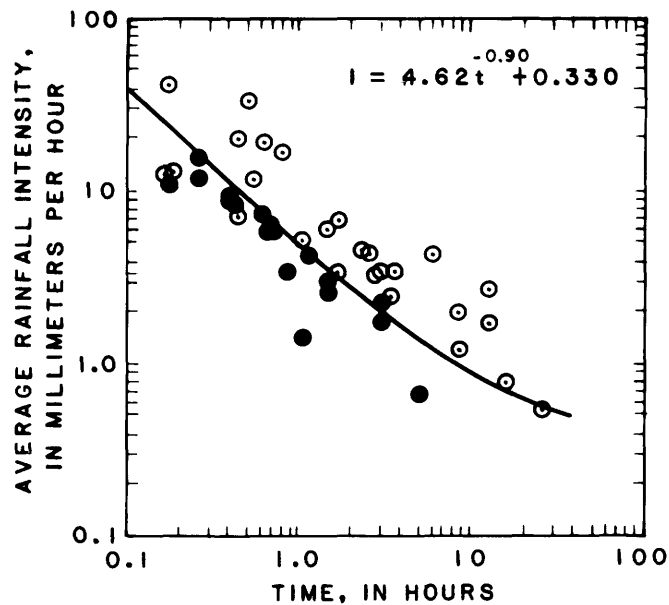


Figure 7.--Incipient-ponding curve and equation, Dead Horse Creek tributary No. 2 near Midwest, Wyoming (06312920).

Sensitivity of Parameters

Information on model response to changes in parameter values is useful in understanding the model. A mathematical fit of the data using some fitting criteria is necessary to determine sensitivity of the parameters. Unfortunately a mathematical fitting scheme for the separation curve was not available and the best fit had to be determined visually. Therefore, a graphical approach to the sensitivity test was used. Values of plus 10, 20, and 30 percent and minus 10, 20, and 30 percent from the optimum parameter values were used for each parameter and plotted on a graph with the data points. The best-fit curve and the curves of plus 30 percent and minus 30 percent for each parameter for Dugout Creek tributary near Midwest, Wyo. (06313180) are shown in figure 8. Similar plots were made for Dead Horse Creek tributary near Midwest, Wyo. (06312910) and Dead Horse Creek tributary No. 2 near Midwest, Wyo. (06312920) but are not shown in the report.

Rainfall-intensity and storm-length data from Dugout Creek tributary near Midwest, Wyo. (06313180) were used to evaluate the effects of parameter changes on computed runoff. A 20-percent decrease in computed runoff resulted from a plus 30-percent change in parameter a , and a 22-percent increase in computed runoff resulted from a minus 30-percent change in parameter a . The plus 30-percent change in parameter n resulted in 4-percent decrease, and minus 30-percent change in parameter n resulted in 9-percent increase in computed runoff. Percent changes in computed runoff for changes in parameter n are also a function of the distribution of the rainfall-intensity and storm-length data points around the equation intercept ($t =$ one hour), therefore parameter n is difficult to evaluate. A plus 30-percent change in parameter f_c caused a 7-percent decrease in computed runoff, and a minus 30-percent change in f_c caused a 5-percent increase in computed runoff.

Test of Constant Rainfall Rate

Tests were made to evaluate the effects of the assumption of the constant rainfall rate, which does not occur in nature. Two assumed storm events, each with an average intensity of 15 mm/h and a storm length of 1.36 hours, were used in the analyses. The first event had one-third of the total precipitation in the first half of the storm, time t_1 to t_2 , and two-thirds of the total precipitation in the second half of the storm. Total storm length was two times t_1 . The second storm event had the same storm length as the first event but had two-thirds of the total precipitation in the first half of the storm and one-third of the precipitation in the second half of the event. Runoff was computed for the two assumed storms and for the mean of the two events. The same incipient-ponding curve was used for all computations. A second set of assumed storm events with an average intensity of 4.50 mm/h and a storm length of 7.32 hours was used to check lower intensity events. The same methods were used for this set of storms as were used in the first.

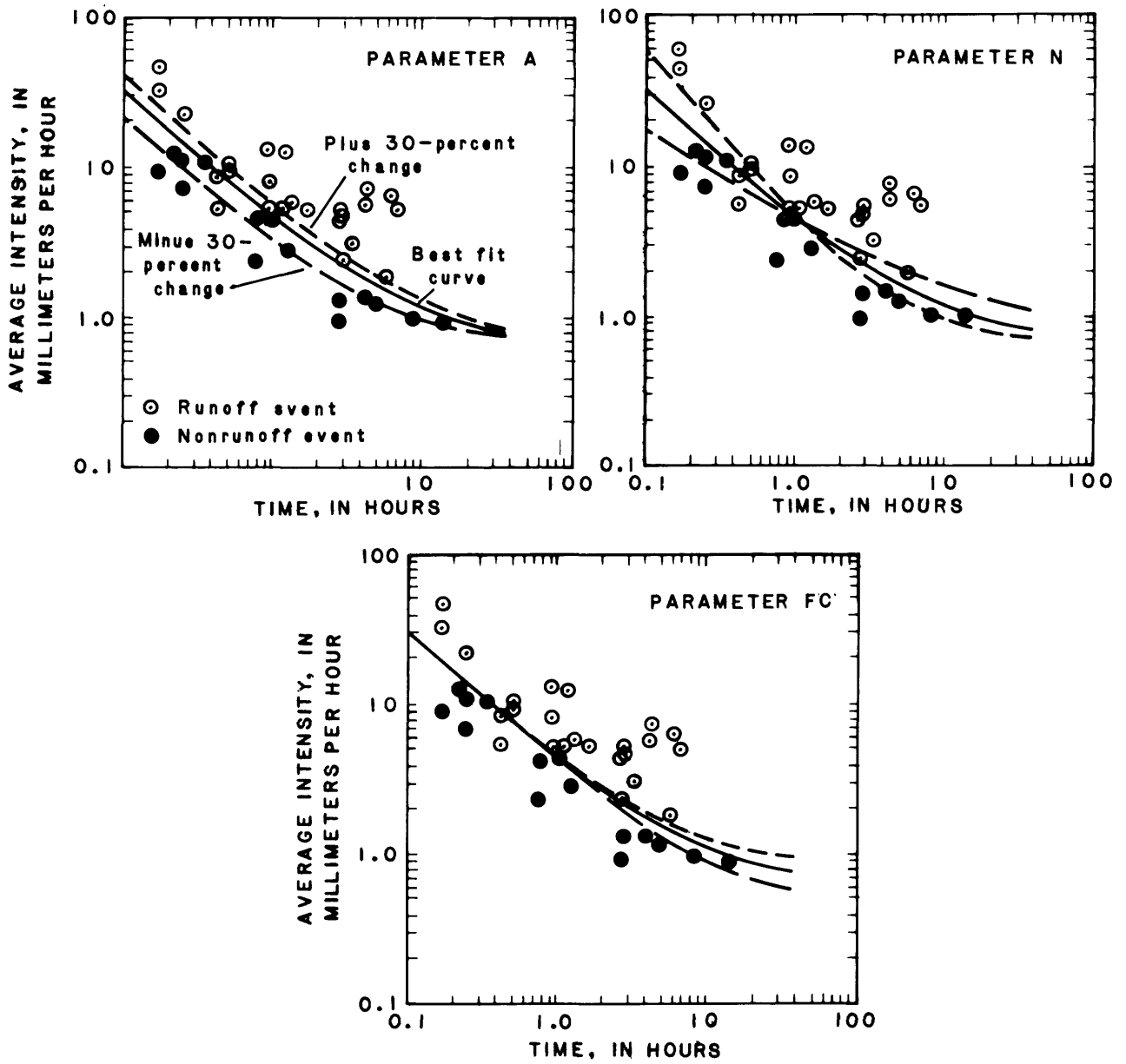


Figure 8.--Incipient-ponding curves for changes in indicated parameters; Dugout Creek tributary near Midwest, Wyoming (06313180).

Results of the analysis of both storm sets show that when the low-intensity part of the storm was in the first half of the event the computed runoff was about 8 percent higher than the runoff computed from the mean, and when the high-intensity part of the storm came first the computed runoff was about 3 percent lower than the runoff computed for the mean. A small bias has been introduced by using the assumption of constant rainfall rate, but the error introduced is small when compared to the accuracy of the overall method.

The one-third and two-thirds ratio of the total precipitation for the two storm parts was an arbitrary selection, but later studies indicated that this closely approximates precipitation ratios in actual storms in the Powder River Basin. Eighty-three rain storms from four precipitation gages in northeastern Wyoming were analyzed to determine the average distribution ratio. The ratio was three-tenths and seven-tenths compared to the one-third and two-thirds ratio used in this report.

BASINS WITH MULTIPLE-SOIL COMPLEXES

Small basins with a single-soil complex and a single incipient-ponding curve are rare. Most of the small basins in the Powder River Basin have several soil complexes. Because the soil complexes vary from tight clay, clay loams, and sandy loams to sand, infiltration rates range from very low to very high.

When using the separation technique to define an incipient-ponding curve, only the incipient-ponding curve for the soil with the lowest infiltration rate can be defined in a multiple-soil basin. Therefore, a method is needed that will evaluate incipient-ponding curves for soil complexes with infiltration rates greater than the one with the lowest rate.

Infiltration rates of soils can be ranked in ascending order by first determining the relative permeability using methods described in U.S. Department of Agriculture (1962, p. 168), which states, "In the absence of precise measurements, soils may be placed into relative permeability classes through studies of structure, texture, porosity, cracking, and other characteristics of the horizons in the soil profile in relation to local use experience." The next step is to define the area of each soil complex in the basin and to rank the soils in ascending order of their relative infiltration rates.

A storm with an average intensity greater than the infiltration rate of the soil complex with the lowest permeability, but with an intensity less than the infiltration rates of the soil complexes of the remainder of the basin, will produce runoff only from one soil complex. The infiltration rates of all the soil complexes in a basin can be evaluated by using a number of storms with a range in average intensities from just greater than the lowest infiltration rate to intensities greater than the highest infiltration rate. A schematic model of the method used to define subbasin incipient-ponding curves is shown in figure 9.

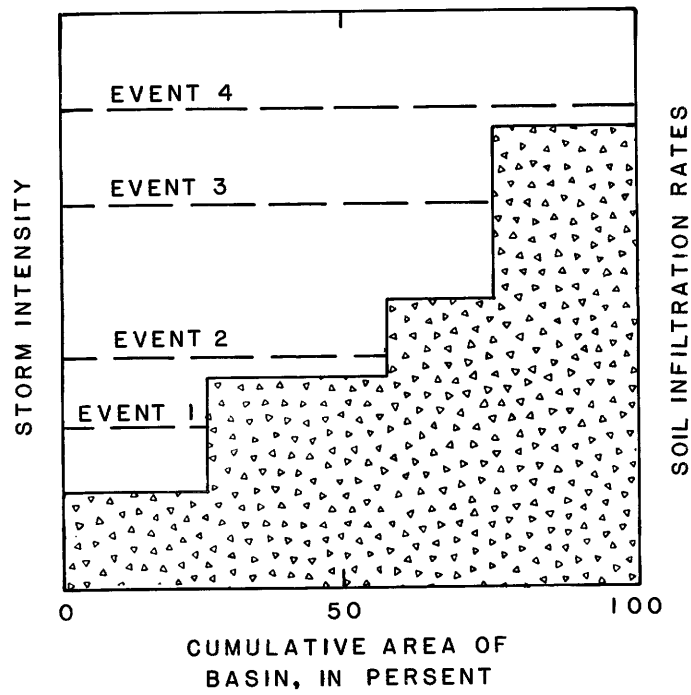


Figure 9.--Schematic model of subbasin infiltration rates.

A unique solution is possible by assuming a series of incipient-ponding curves parallel to the lowest incipient-ponding curve and using them to compute the runoff for the basin subarea. The runoffs from the basin subareas are summed to obtain the total runoff for the event. Each simulated runoff event is compared to the measured value of runoff. This process is repeated until the difference between simulated runoff and measured runoff is some acceptable sum of the least-squares fit of all the events for the basin. Infiltration rates are determined by the fitting process for each soil subarea while the original order based on permeability of soils is maintained.

The large number of trials required to obtain an acceptable fit is nearly impossible without the aid of a computer and an optimization technique. A modified Rosenbrock optimization technique used by Dawdy and others (1972) for rainfall-runoff studies was adapted to aid in the data fit. Upper and lower constraints were set on the infiltration parameters to keep the ranking of permeabilities of soil complexes in the correct order.

The assumption that the incipient-ponding curves are parallel to the lowest or base incipient-ponding curve was made to reduce the number of parameters needed to fit the incipient-ponding curve for each soil from 3 to 1. This assumption may have some effect on the accuracy of the results, but it should be minor. There is some basis for this assumption, in that the soil complexes in most small basins consist of common soils and soil associations. Some of the soil complexes are different from other soil complexes by only one soil type or the percentages of the soil types in the complex.

SOIL-COMPLEX RANKING

Ranking the soil complexes and associations by relative values of permeability was accomplished in three steps: (1) A relative permeability value for each individual soil was determined, (2) compositions of soil complexes or associations were determined from soil-mapping descriptions, and (3) a composite relative-permeability index was computed for the soil complex or association.

To be useful for calculations, relative classes of soil permeability used by the U.S. Soil Conservation Service must be equated to a single value instead of a class range of values. The class ranges used by Stephens (1975) are listed in table 5. A midpoint for each class was computed by determining the logarithmic values of the end points and taking the antilog of their mean. This computation reduces the class range to a single value for relative soil permeability. These values are also listed in table 5.

Each soil complex or association described by the Soil Conservation Service gives the soil types and percentages of the component parts. By use of relative class permeability for a soil type and the percentage of the soil in the complex, a composite value can be computed. A sample computation for the Terry-Tulloch-Valent soil complex is shown in table 6.

Table 5.--Relative class values of soil permeability

Class description	Numerical class (mm/h)	Relative soil permeability (mm/h)
1 Very slow	Less than 1.52	¹ 1.52
2 Slow	1.52 to 5.08	2.78
3 Moderately slow	5.08 to 15.2	8.76
4 Moderate	15.2 to 50.8	27.8
5 Moderately rapid	50.8 to 152.4	88.0
6 Rapid	152.4 to 508.0	278

¹ Upper end point was used.

Table 6.--Sample computation to determine composite relative-permeability index for the Terry-Tullock-Valent soil complex

Soil name	Percentage of total	Relative soil permeability (mm/h)	Weighted incremental soil permeability (mm/h)
Terry	35	88.0	30.8
Tullock	30	88.0	26.4
Valent	20	278.0	55.6
Vona	5	88.0	4.4
Tassel	5	88.0	4.4
Lesset	5	88.0	4.4
			¹ 126.0

¹ Sum of weighted values.

Table 7.--Mapping units for soil maps and associated permeabilities

Mapping unit	Soil complex or association	Composite soil permeability (mm/h)	Percentage of area (fig. 10)		
			Basin A	Basin B	Basin C
80B	Samsil-Shingle-Worf Complex	14.5	----	1.2	----
115AB	Undifferentiated Flood Loams	27.9	----	----	0.5
163A	Kim-Limon Association	20.3	9.5	----	----
177C	Thedalund-Kim Association	24.4	----	2.3	----
179C	Ulm-Renohill Complex	20.1	23.3	----	----
207D	Shingle-Worf Complex	27.9	----	----	1.3
226DE	Samsil-Shingle-Rockland Complex	6.6	----	----	48.3
244BC	Cushman-Briggsdale Association	54.4	----	----	2.5
248AB	Stoneham-Kim Association	27.9	----	----	.5
249BC	Briggsdale-Renohill Association	27.2	----	----	8.9
250BC	Renohill-Razor Association	2.8	----	----	9.0
264D	Cushman-Shingle-Worf Association	30.7	----	----	3.1
266CD	Ascalon-Olney Association	27.9	----	----	3.1
285CD	Samsil-Gaynor-Razor Complex	2.5	----	----	9.4
322C	Terry-Tullock-Valent Complex	126.0	5.2	10.6	----
332C	Cushman-Terry Association	81.8	----	5.9	----
336C	Fort Collins-Cushman Association	51.8	1.9	----	----
344C	Stoneham-Cushman Association	46.0	----	----	2.2
364D	Thedalund-Shingle-Gaynor Complex	13.0	----	----	8.8
365C	Shingle-Thedalund Association	20.3	----	----	.2
380C	Olney-Bowbac Complex	27.9	33.2	32.0	----
384C	Olney-Vona Association	46.0	----	18.4	----
393C	Renohill-Worfka-Shingle Complex	13.5	10.2	----	----
402C	Shingle-Lesset-Tassel Complex	54.4	2.6	1.8	----
404C	Tassel-Tullock-Vona Complex	87.9	9.0	27.8	----
405D	Tassel-Terry-Rockland Complex	75.9	5.1	----	----
GA42C	Zigwield Loam	27.9	----	----	.5
H78B	Cushman Fine Sandy Loam	87.8	----	----	.3
K33C	Olney Fine Sandy Loam	27.9	----	----	1.4
NC	Noncontributing Area	----	----	----	----

ANALYSIS OF DATA FOR MULTIPLE-SOIL COMPLEXES

Soil maps, descriptions of soils, and rainfall-runoff data are available for three small basins in the Powder River Basin--Sage Creek tributary near Orpha, Wyo. (06648780); Frank Draw tributary near Orpha, Wyo. (06648720); and Headgate Draw at upper station near Buffalo, Wyo. (06316480). Soil-mapping units were outlined on aerial photographs and then transferred to topographic maps. Soil-mapping units were planimetered to determine the area of each unit in the basin, and the composite relative permeability for each soil complex was computed. Maps of the soil units are shown in figure 10. The mapping units for the soil complexes or associations, percentage of area, and the associated permeability are listed in table 7.

Incipient-ponding curves for the soil complexes or associations with the lowest infiltration rate were defined by using the rainfall and runoff data and by constructing the separation lines. The lowest incipient-ponding curves and equations for the three multiple-soil basins are shown in figures 11, 12, and 13.

Incipient-ponding curves for each soil complex with an infiltration rate greater than the lowest rate were optimized using rainfall data and their associated runoff data. The infiltration rate for each soil maintained a set position relative to those for other soils in the basin. A set of incipient-ponding curves was optimized for each basin. The storm-intensity data points and the incipient-ponding curves are shown for Frank Draw (fig. 14) and Sage Creek (fig. 15) tributaries near Orpha, Wyo.

Four soil complexes or associations are common to both the Frank Draw tributary and the Sage Creek tributary basins. Graphical comparisons of the optimized incipient-ponding curves of the four soils for the two basins are presented in figure 16. The largest numerical difference, 32 percent, between optimized incipient-ponding curves is for the Tassel-Tulloch-Vona complex. An average of the two curves would provide the best answer for the data available but has not been presented in this report.

Headgate Draw basin has 16 mapped soil complexes and associations, of which 11 make up only 15.6 percent of the total basin area. With only 11 usable storm events available to optimize an incipient-ponding curve for the basin, it was necessary to combine soil areas. Soil-mapping units were combined on the basis of similar relative-permeability indexes, soil descriptions, and the area of the soil subunits. Six soil groups were optimized. Two of the six soil groups optimized to the same values as those for two of the other soil groups, resulting in four incipient-ponding curves representing all the soil complexes of the basin. The incipient-ponding curves for the soil groups with the highest infiltration rates can be defined only as greater than the value obtained from the highest rainfall event. Rainfall events with higher intensities and longer durations are needed to define the soil groups with the highest infiltration rates. The storm-intensity data points and the incipient-ponding curves for Headgate Draw at upper station near Buffalo, Wyo. are shown in figure 17.

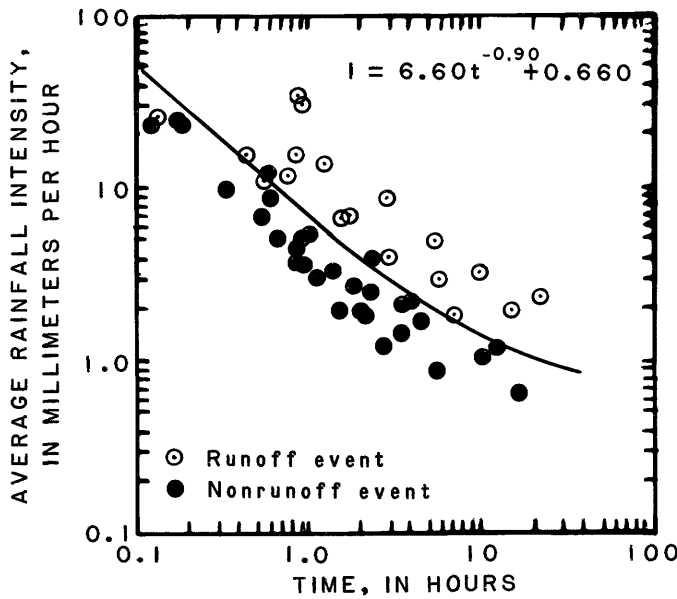


Figure 11.--Lowest incipient-ponding curve and equation, Frank Draw tributary near Orpha, Wyoming (06648720).

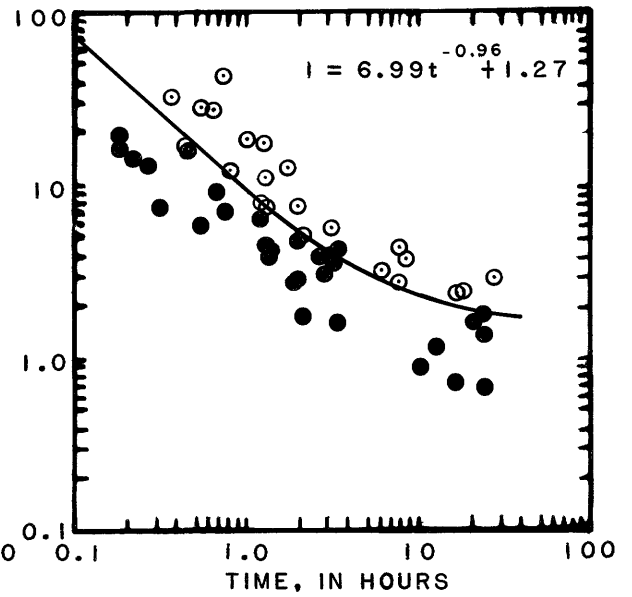


Figure 12.--Lowest incipient-ponding curve and equation, Sage Creek tributary near Orpha, Wyoming (06648780).

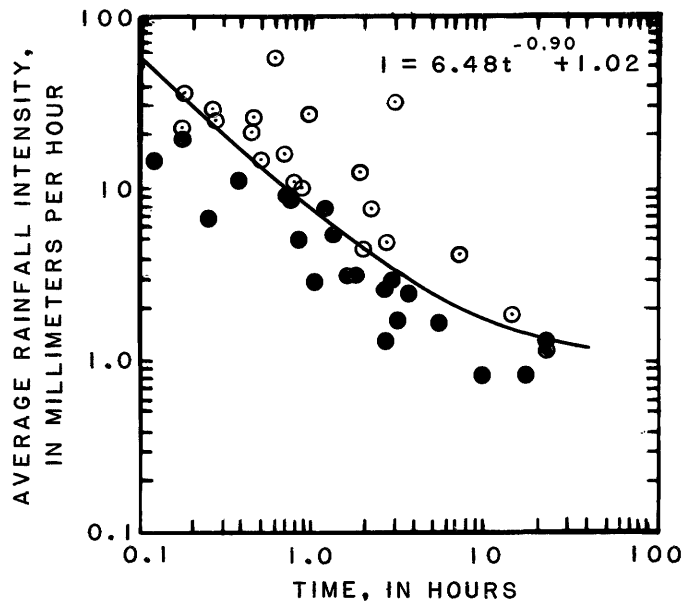


Figure 13.--Lowest incipient-ponding curve and equation, Headgate Draw at upper station near Buffalo, Wyoming (06316480).

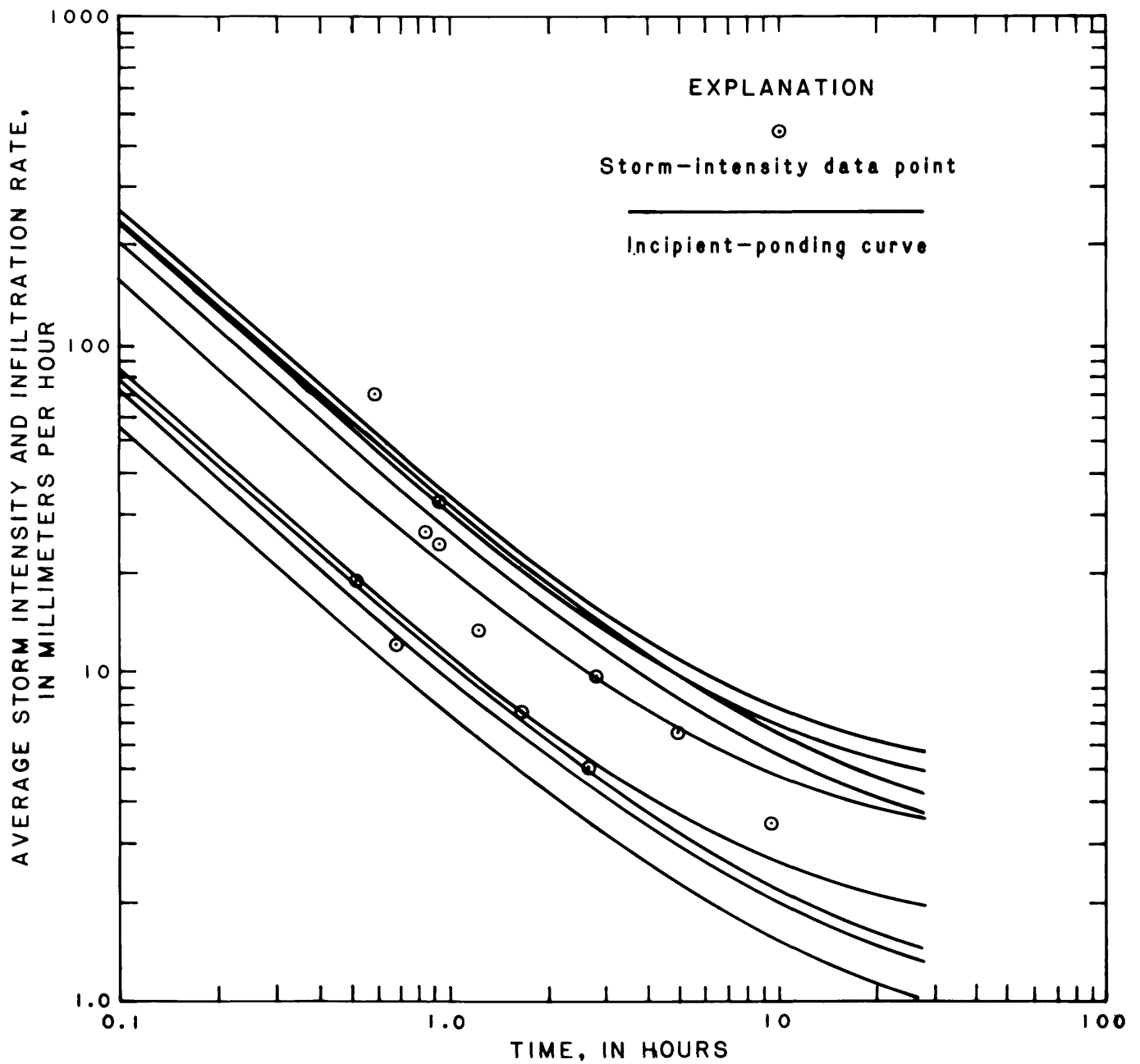


Figure 14.--Incipient-ponding curves for Frank Draw tributary near Orpha, Wyoming (06648720).

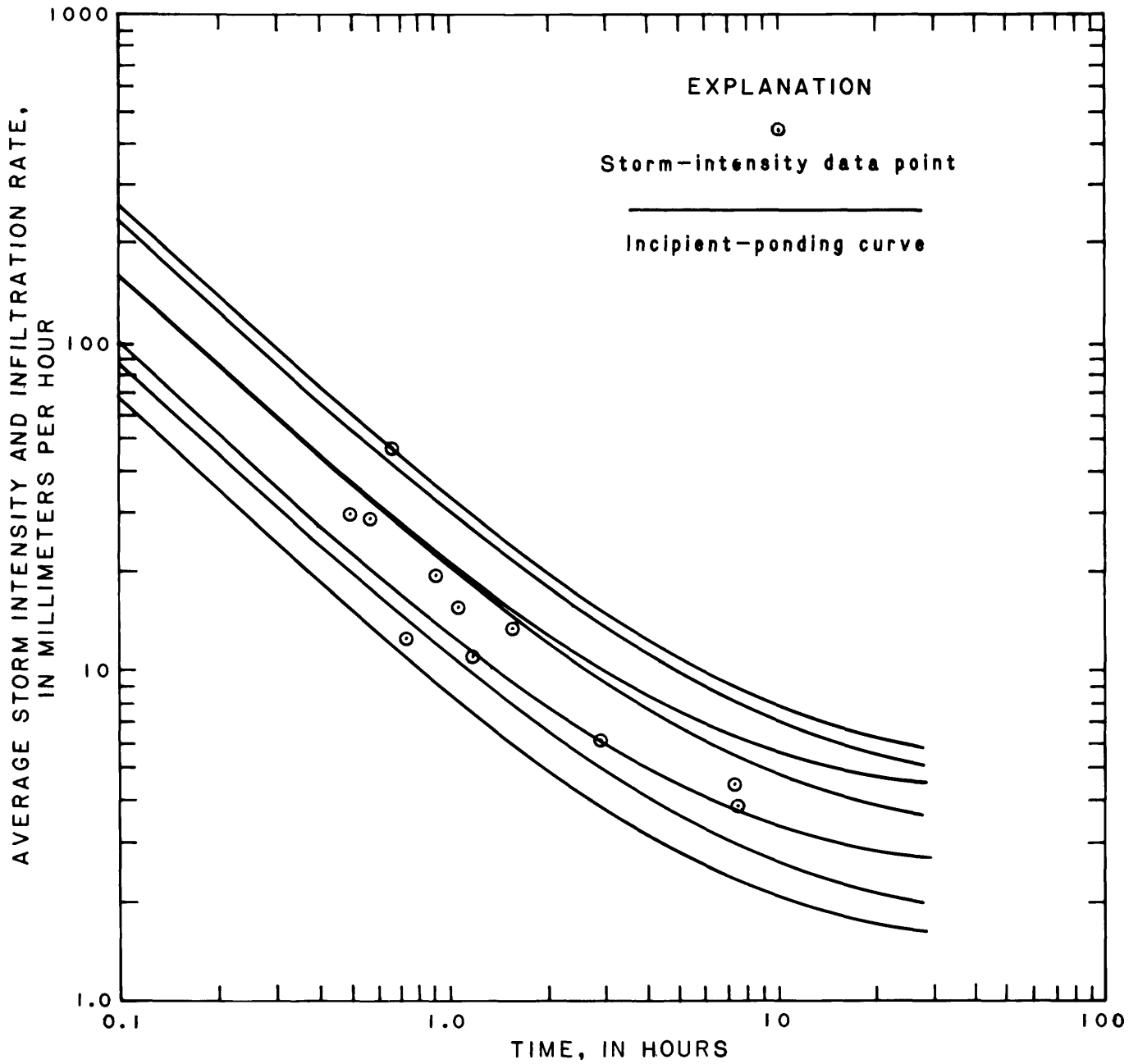


Figure 15.--Incipient-ponding curves for Sage Creek tributary near Orpha, Wyoming (06648780).

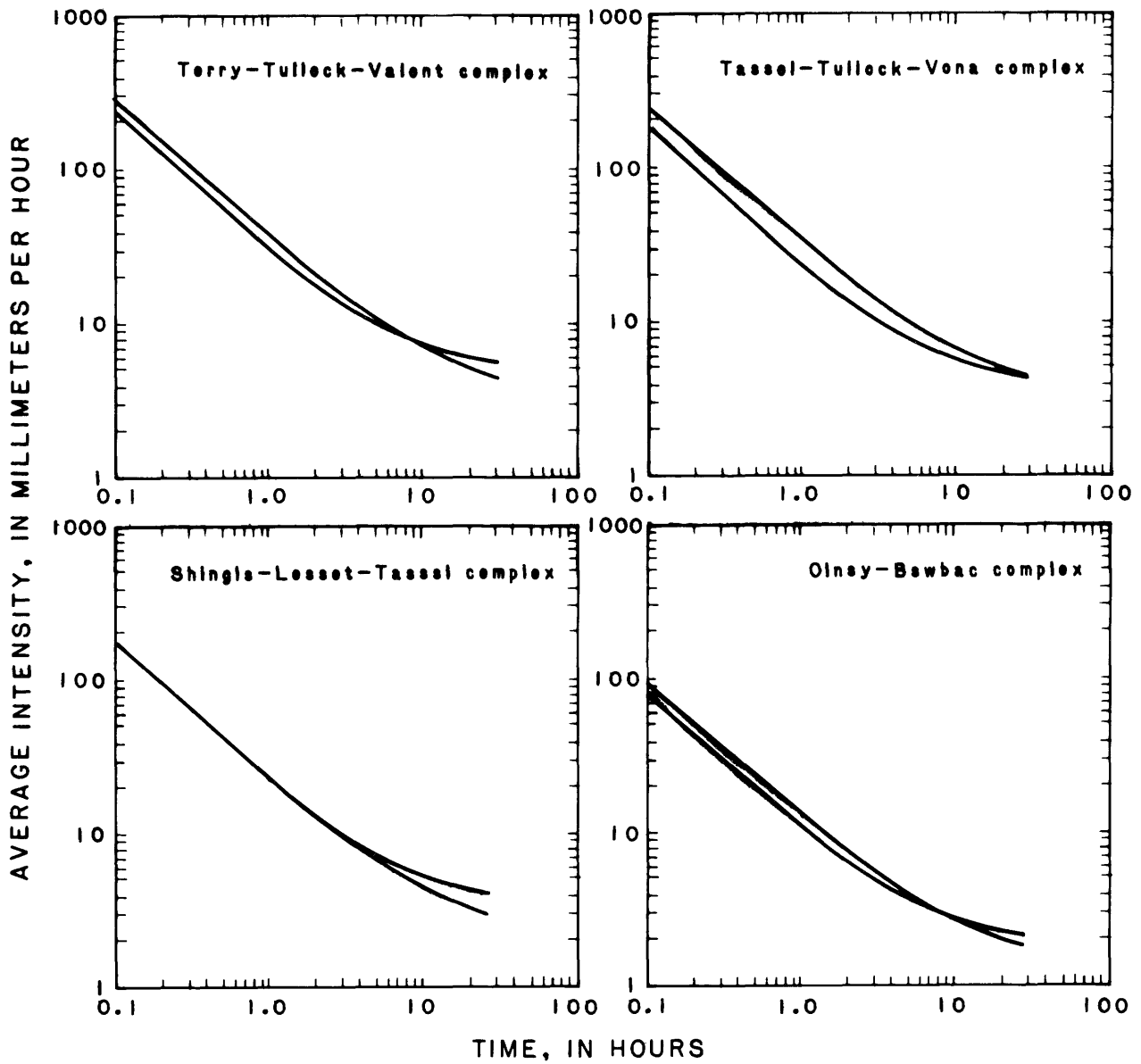


Figure 16.--Optimized incipient-ponding curves for soils common to both Frank Draw tributary near Orpha, Wyoming (06648720) and Sage Creek tributary near Orpha, Wyoming (06648780).

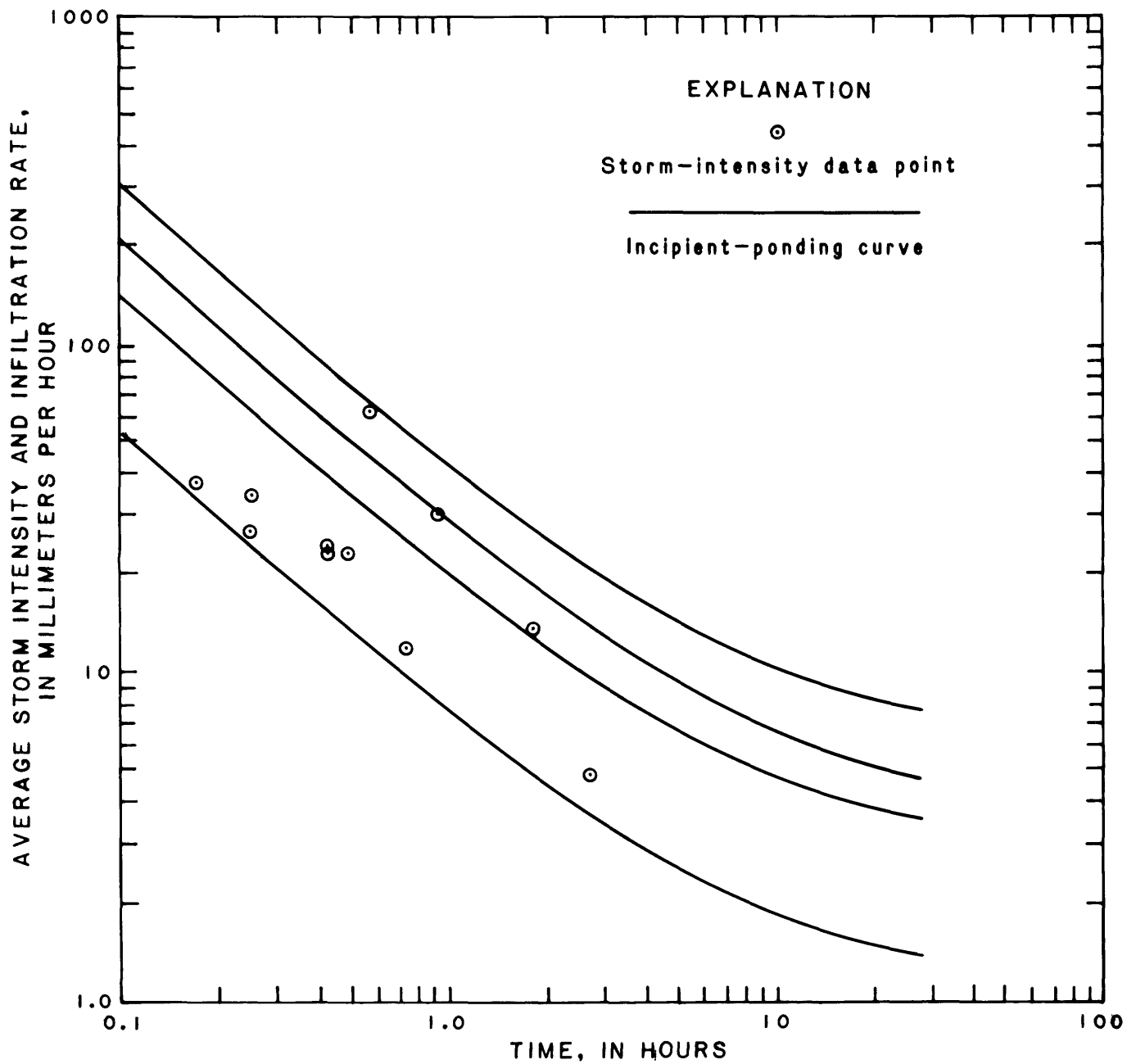


Figure 17.--Incipient-ponding curves for Headgate Draw at upper station near Buffalo, Wyoming (06316480).

Parameter values for incipient-ponding curves for all soil complexes and associations investigated in this study are listed in table 8. The four soil associations in the Headgate Draw basin with the highest infiltration rates are flagged to indicate that the correct values may be greater than those listed.

The date, total rainfall, storm duration, storm intensity, measured runoff, and simulated runoff of each event are listed for Frank Draw tributary near Orpha, Wyo. (06648720) in table 9, Sage Creek tributary near Orpha, Wyo. (06648780) in table 10, and Headgate Draw at upper station near Buffalo, Wyo. (06316480) in table 11.

Total simulated runoff was compared to total measured runoff for each of the multiple-soil basins. The standard deviations were computed using equations 16 and 17. Comparisons of computed runoff to measured runoff for small basins with multiple soils are summarized in table 12.

Because of the small sample size in relation to the number of soils in a basin (parameters), the numerical comparisons made in table 12 have little or no statistical significance but are presented to show the data fit. Sufficient data are needed to perform a split sample test to prove the multiple-soil method presented in this report. A similar test can be made using two basins with the same soil types where data from one basin can be used to calibrate the soil parameters and the data from the other basin can be used as a test sample. A continuing program on infiltration should provide the necessary data.

LONG-TERM COMPARISON

A long-term rainfall-runoff record would provide the necessary information to make a valid statistical evaluation of the incipient-ponding method and of the stated assumptions. Unfortunately, long-term rainfall-runoff records are not available, but long-term rainfall and simulated runoff records from a rainfall-runoff model (Craig and Rankl, 1978) are available for the basins used in this study.

Average storm intensity and storm length were computed from unit-precipitation data obtained from the U.S. Weather Bureau station, Cheyenne, Wyo., for the period from 1901-73. The seasonal storm which produced the largest seasonal runoff event for the rainfall-runoff model was used for the incipient-ponding method. A rainfall-intensity adjustment described by Craig and Rankl (1978) was used to adjust the Cheyenne record to the basins of interest.

Using the adjusted rainfall records with the incipient-ponding method, 73 years of seasonal runoff events were simulated. A log-Pearson Type III distribution was applied to the data to describe runoff-frequency curves. These frequency curves and those from the rainfall-runoff model for each of the study basins are shown in figure 18.

The runoff results from the two models were compared as a check on the infiltration model; neither model seemed better than the other. A statistical test was made on the hypothesis that there is no difference between the mean log values of the volume-runoff parameter for the two simulation methods. A paired-difference test was used for each basin; the hypothesis could not be rejected at the 0.05 level of significance.

Table 8.--Soil parameters for incipient-ponding curves
in the Powder River Basin

Soil complex or association	<u>Incipient-ponding equation</u>		
	a	n	f _c
<u>Frank Draw tributary near Orpha, Wyo. (06648720)</u>			
Renohill-Worfka-Shingle Complex	I= 6.60T**	(-0.90)	+0.66
Ulm-Renohill Complex	I= 8.51T**	(-0.90)	+0.85
Kim-Limon Association	I= 9.37T**	(-0.90)	+0.94
Olney-Bowbac Complex	I=11.88T**	(-0.90)	+1.19
Shingle-Lesset-Tassel Complex	I=17.99T**	(-0.90)	+1.80
Fort Collins-Cushman Association	I=24.40T**	(-0.90)	+2.44
Tassel-Terry-Rockland Complex	I=28.99T**	(-0.90)	+2.90
Tassel-Tullock-Vona Complex	I=30.32T**	(-0.90)	+3.03
Terry-Tullock-Valent Complex	I=32.62T**	(-0.90)	+3.26
<u>Sage Creek tributary near Orpha, Wyo. (06648780)</u>			
Samsil-Shingle-Worf Complex	I= 6.99T**	(-0.96)	+1.27
The dalund-Kim Association	I= 6.99T**	(-0.96)	+1.27
Olney-Bowbac Complex	I= 9.09T**	(-0.96)	+1.65
Olney-Vona Association	I=11.67T**	(-0.96)	+2.12
Shingle-Lesset-Tassel Complex	I=17.05T**	(-0.96)	+3.10
Cushman-Terry Association	I=17.07T**	(-0.96)	+3.10
Tassel-Tullock-Vona Complex	I=20.41T**	(-0.96)	+3.70
Terry-Tullock-Valent Complex	I=25.37T**	(-0.96)	+4.61
<u>Headgate Draw at upper station near Buffalo, Wyo. (06316480)</u>			
Samsil-Gaynor-Razor Complex	I= 6.48T**	(-0.90)	+1.02
Renohill-Razor Association	I= 6.48T**	(-0.90)	+1.02
Samsil-Shingle-Rockland Complex	I=16.71T**	(-0.90)	+2.62
The dalund-Shingle-Gaynor Complex	I=16.71T**	(-0.90)	+2.62
Shingle-The dalund Association	I=16.71T**	(-0.90)	+2.62
Briggsdale-Renohill Association	I=24.31T**	(-0.90)	+3.40
Shingle-Worf Complex	I=24.31T**	(-0.90)	+3.40
Stoneham-Kim Association	I=24.31T**	(-0.90)	+3.40
Olney Fine Sandy Loam	I=24.31T**	(-0.90)	+3.40
Ascalon-Olney Association	I=24.31T**	(-0.90)	+3.40
Zigwield Loam	I=24.31T**	(-0.90)	+3.40
Undifferentiated Flood Loams	I=24.31T**	(-0.90)	+3.40
Stoneham-Cushman Association ¹	I=28.96T**	(-0.90)	+4.55
Cushman-Shingle-Worf Association ¹	I=28.96T**	(-0.90)	+4.55
Cushman-Briggsdale Association ¹	I=28.96T**	(-0.90)	+4.55
Cushman Fine Sandy Loam ¹	I=28.96T**	(-0.90)	+4.55

¹ Infiltration rates may be greater than the values listed.

Table 9.--Precipitation and runoff data for Sage Creek tributary near Orpha, Wyo. (06648780)

Date	Rainfall (mm)	Length of storm (h)	Intensity (mm/h)	Measured runoff (mm)	Simulated runoff (mm)
06-10-65	12.95	1.17	11.07	0.38	0.18
06-14-65	9.40	.75	12.53	.28	.00
06-16-65	16.51	.58	28.47	1.60	1.19
07-25-65	30.23	.66	45.80	7.69	7.49
08-19-66	14.48	.50	28.95	.84	.71
06-15-67	29.46	7.66	3.85	1.02	1.22
06-12-70	32.51	7.50	4.33	.84	2.21
05-30-71	17.53	.92	19.05	1.32	1.27
08-02-72	20.83	1.58	13.18	1.35	1.85
07-22-73	16.51	1.08	15.29	1.85	.91
09-09-73	17.27	2.92	5.91	.66	.36

Table 10.--Precipitation and runoff data for Frank Draw tributary near Orpha, Wyo. (06648720)

Date	Rainfall (mm)	Length of storm (h)	Intensity (mm/h)	Measured runoff (mm)	Simulated runoff (mm)
05-23-65	26.92	2.75	9.79	4.93	6.38
06-10-65	12.70	2.58	4.92	2.39	.18
06-24-65	22.35	.83	26.93	7.29	5.69
08-19-66	41.15	.58	70.95	14.88	20.93
06-15-67	33.02	9.50	3.48	5.72	5.03
07-15-68	22.61	.92	24.58	3.33	5.72
06-11-69	16.26	1.21	13.44	.41	1.70
05-30-71	30.23	.92	32.85	12.01	11.05
08-02-72	10.16	1.67	6.08	.15	.05
07-30-73	31.75	4.92	6.45	9.09	7.62
08-11-73	9.40	.50	18.80	.94	.15
08-12-73	8.13	.67	12.13	4.29	.03

Table 11.--Precipitation and runoff data for Headgate Draw at upper station
near Buffalo, Wyo. (06316480)

Date	Rainfall (mm)	Length of storm (h)	Intensity (mm/h)	Measured runoff (mm)	Simulated runoff (mm)
08-15-68	6.35	0.25	25.40	0.10	0.00
08-23-68	12.70	2.67	4.76	.15	.18
07-16-69	35.31	.58	60.88	10.16	11.66
05-23-70	11.43	.50	22.86	.13	.46
06-19-70	26.92	.92	29.26	6.12	4.65
06-29-70	6.10	.17	35.88	.05	.00
07-08-70	8.38	.25	33.52	.13	.15
07-10-70	9.40	.42	22.38	.71	.20
06-03-72	24.13	1.83	13.19	1.78	2.21
07-23-72	8.64	.75	11.52	.15	.08
09-11-72	9.14	.42	21.76	.20	.18

Table 12.--Comparison of computed runoff to measured runoff for
small basins with multiple soils

Basin name and number	Number of events	Total rainfall (mm)	Measured runoff (mm)	Computed runoff (mm)	Percent difference	Standard deviation
Frank Draw tributary near Orpha, Wyo. (06648720).	12	267.5	65.4	64.5	-1.4	2.75
Sage Creek tributary near Orpha, Wyo. (06648780).	11	217.7	17.8	17.6	-1.1	.67
Headgate Draw at upper station near Buffalo, Wyo. (06316480).	11	158.5	19.7	19.7	0	.74

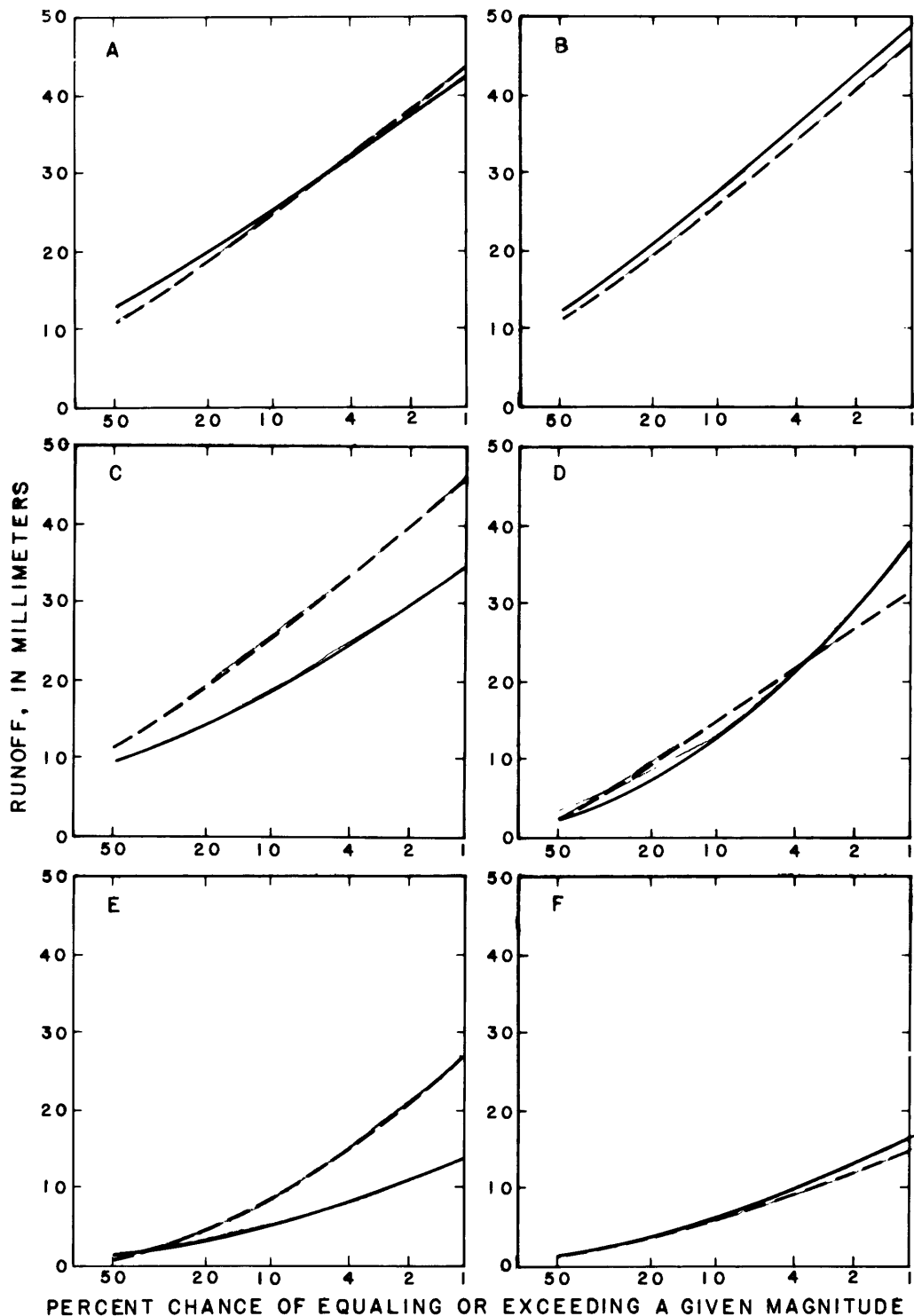


Figure 18.--Long-term simulation data using the incipient-ponding method (dashed line) and the rainfall-runoff model (solid line) for A, Dugout Creek tributary near Midwest, Wyo. (06313180); B, Dead Horse Creek tributary near Midwest, Wyo. (06312910); C, Dead Horse Creek tributary No. 2 near Midwest, Wyo. (06312920); D, Frank Draw tributary near Orpha, Wyo. (06648720); E, Sage Creek tributary near Orpha, Wyo. (06648780), and F, Headgate Draw at upper station near Buffalo, Wyo. (06316480).

SUMMARY

An empirical infiltration model that can be used to estimate the volume of storm runoff has been applied to small ephemeral drainage basins in Wyoming. Data required to compute runoff are the areas of soil complexes or associations for the drainage basin, three infiltration parameters for each soil complex or association, and a design storm consisting of rainfall intensity and duration.

The infiltration model uses incipient-ponding curves to determine the infiltration parameters of soils from limited rainfall and runoff data in a semiarid climate. An infiltration equation based on the incipient-ponding equation was used to compute the water uptake after ponding. These two equations were used to define the soil parameters for six small drainage basins in Wyoming.

Three assumptions were made in order to use the incipient-ponding concept for the study: (1) The initial infiltration includes interception, surface storage, and channel storage; (2) antecedent moisture conditions for a storm are some long-term average; and (3) rainfall for a storm is uniform in both time and space.

For basins with multiple-soil complexes or associations, a modified Rosenbrock optimization technique was used to fit incipient-ponding curves for soils with infiltration rates greater than the base curve.

Statistical comparisons were made between measured runoff and simulated runoff. Values for the six basins studied ranged from -16.6 to 2.3 percent difference between total measured runoff and total simulated runoff for all events used. A scatter of the fit was analyzed by computing the standard deviation of the data for each site. These values ranged from 0.67 to 3.50. A comparison was made between long-term simulated records obtained from a rainfall-runoff model and a long-term simulated record computed from rainfall records using the incipient-ponding model. A paired-difference test shows no significant difference between the two simulation methods.

REFERENCES CITED

- Craig, G. S., Jr., and Rankl, J. G., 1978, Analysis of runoff from small drainage basins in Wyoming: U.S. Geological Survey Water-Supply Paper 2056, 70 p.
- Dawdy, D. R., Lichty, R. W., and Bergmann, J. M., 1972, A rainfall-runoff simulation model for estimation of flood peaks for small drainage areas: U.S. Geological Survey Professional Paper 506-B, 20 p.
- Linsley, R. K., Kohler, M. A., and Paulhus, J. L., 1958, Hydrology for engineers: New York, McGraw-Hill Book Co., 340 p.
- Musgrave, G. W., and Holtan, H. N., 1964, Infiltration, in Chow, V. T., ed., Handbook of applied hydrology: New York, McGraw-Hill Book Co., sec. 12, p. 12-1--12-30.
- Rubin, Jacob, 1966, Theory of rainfall uptake by soils initially drier than their field capacity and its applications: Water Resources Research, v. 2, no. 4, p. 739-749.
- Smith, R. E., 1972, The infiltration envelope: Results from a theoretical infiltrometer: Journal of Hydrology, v. 17, p. 1-22.
- Smith, R. E., and Chery, D. L., Jr., 1973, Rainfall excess model from soil water flow theory: American Society of Civil Engineers Proceedings, v. 99, no. HY 9, p. 1337-1351.
- Stephens, J. R., Jr., 1975, Soil survey of Johnson County, Wyoming, southern part: U.S. Department of Agriculture, Soil Conservation Service, 156 p.
- Swartzendruber, D., and Hillel, D., 1975, Infiltration and runoff for small field plots under constant intensity rainfall: Water Resources Research, v. 11, no. 3, p. 445-451.
- U.S. Department of Agriculture, 1962, Soil survey manual: U.S. Department of Agriculture Handbook 18, 487 p.